Thesis for the Degree of Master of Philosophy

Studies on properties and ligand interactions of cluster II and IV of low-density lipoprotein receptor-related protein 1 (LRP1) expressed in *Escherichia coli*

by

Ye Seul Seo

Department of Chemistry

The Graduate School

Pukyong National University

February 23, 2018

Studies on properties and ligand interactions of cluster II and IV of low-density lipoprotein receptor-related protein 1 (LRP1) expressed in *Escherichia coli*

(대장균에서 발현한 저밀도 지단백질 수용체 관련 단백질 1 (LRP1) cluster II와 IV의 특성 및 리간드 상호작용에 대한 연구)

Advisor: Prof. Hak Jun Kim

by

Ye Seul Seo

A thesis submitted in partial fulfillment of the requirements

for the degree of Master of Philosophy

in Department of Chemistry, The Graduate School,

Pukyong National University

February 2018

Studies on properties and ligand interactions of cluster II and IV
of low-density lipoprotein receptor-related protein 1 (LRP1) expressed in *Escherichia coli*

A dissertation

by

Ye Seul Seo

Approved by:

_____

Prof. Myung Won Lee (Chairman)

_____ _____

Prof. Hak Jun Kim (Member) Prof. Sangwook Wu (Member)

February 23, 2018

Studies on properties and ligand interactions of cluster II and IV of low-density lipoprotein receptor-related protein 1 (LRP1) expressed in *Escherichia coli*

Ye Seul Seo

Department of Chemistry, The Graduate School,
Pukyong National University

Abstract

Low-density lipoprotein receptor-associated protein 1 (LRP1) is an endocytic receptor involved in various types of biological processes with its ligand-binding abilities. The interactions of LRP1 mainly occur on the second and fourth clusters, which consist of several complement-type repeat (CR) domains. Therefore, I expressed clusters II and IV of LRP1 from *Escherichia coli*, an effective host for expressing recombinant proteins with its high yield compared with its cost and culture volume, and studied its properties and interactions through diverse methods, including analytical size-exclusion chromatography (ASEC), analytical ultracentrifugation (AUC), fluorescence emission spectroscopy, circular dichroism (CD) spectroscopy, and surface plasmon resonance (SPR). As a result, I observed their oligomerization, strong Ca^{2+} dependence for structural stability, and low affinity with their ligands. However, these results need to be proved with other *E. coli* strains, vectors, and conditions for induction.

Table of Contents

List of Figures

List of Tables

I. Introduction

1. Low-density lipoprotein receptor-related protein 1 (LRP1)

LRP1, a member of the low-density lipoprotein receptor (LDLR) gene family, is an endocytic multifunctional receptor playing a role in lipid metabolism, the cellular entry of viruses and toxins, the homeostasis of proteinases and proteinase inhibitors, the activation of lysosomal enzymes, embryonic development, various cellular signal transductions, and neurotransmission.[1,2] These diverse functions of LRP1 come from its property of interacting with more than 30 types of structurally unrelated ligands (Table 1).[2,3]

Table 1. Ligands bound to LRP1

Ligands	Roles
ApoE	Lipoprotein metabolism
Lipoprotein lipase	
tPA	Signaling function in brain, fibrinolysis
uPA	Cell migration, healing
Factor IXa	Blood coagulation
Factor VIIIa	
Factor VIIa/TFPI	
MMP-9	Blood coagulation, angiogenesis
MMP-13	Angiogenesis, metastasis
Sphingolipid activator protein (SAP)	
Pregnancy Zone Protein	Proteinase inhibitors, infection
α2M	Proteinase inhibitors, infection

Complement C3	Infection
PAI-1	Regulating tPA/uPA activity
C1 inhibitor	Regulating C1r/C1s activity
Antithrombin III	Regulating blood coagulation
TFPI	Regulating blood coagulation Regulating neutrophil elastase
Heparin cofactor II	
α1-Antitrypsin	
Thrombospondin-1	TGF-β activation, matrix–cell interactions
Thrombospondin-2	Collagen assembly, matrix–cell interactions
Pseudomonas exotoxin A	Collagen assembly, matrix–cell interactions Antibacterial effect
Lactoferrin	
Rhinovirus	Antibacterial effect Chaperone activity
RAP	
HSP-96	Chaperone activity Activation in transcription
HIV-Tat protein	
PDGF	Growth factor

- ApoE, Apolipoprotein E; tPA, tissue-type plasminogen activator; uPA, urokinase plasminogen activator; MMP, matrix metalloproteinase; α_2M, α_2-macroglobulin; PAI-1, plasminogen activator inhibitor 1; TFPI, tissue factor pathway inhibitor; RAP, receptor-associated protein; HSP, heat shock protein; HIV, human immunodeficiency virus; PDGF, platelet-derived growth factor

LRP1, consisting of 4544 amino acids, is synthesized as a single polypeptide chain and cleaved in the terminal cisternae of the trans-Golgi by the intracellular enzyme furin. As a result, a 600-kDa single polypeptide chain is separated into a 515-kDa extracellular fragment and a 85-kDa fragment that contains the transmembrane and cytoplasmic domains. The two subunits are linked by a noncovalent bond.[4,5,6]

LRP1 contains several modular domains: cysteine-rich complement-type repeat (CR) domains,

epidermal growth factor (EGF) domains, β-propeller domains, a transmembrane domain, and a cytoplasmic domain. The CR domains in LRP1 form four clusters containing 2, 8, 10, and 11 CR domains, respectively (Figure 1).[2] These CR domains and their clusters are mainly involved in binding to ligands. Among them, clusters II and IV are mainly involved in ligand bindings, and they have similar affinities with most ligands bound to them.[7] The EGF and β-propeller domains play a major role in ligand uncoupling in the endosomal low-pH environment. The cytoplasmic domain of LRP1 has two dileucine motifs and two terminal NPxY motifs. These terminal NPxY motifs are phosphorylated in tyrosine residues by platelet-derived growth factor receptor-β (PDGFR-β) and connective tissue growth factor (CTGF). The LRP1 cytoplasmic domain interacts with a number of adaptor molecules, including Disables-1 and FE65, which are associated with cellular communication and signal transduction.[3,7,8,9,10]

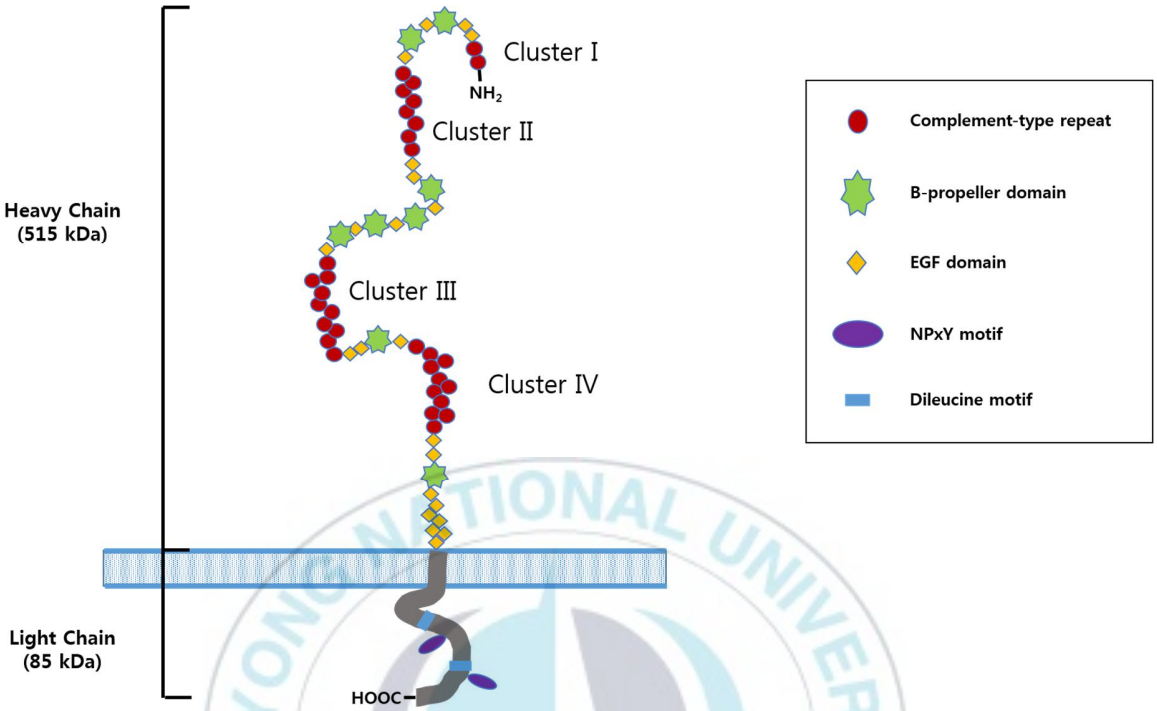

Figure 1. The structure of LRP1

LRP1 is abundantly expressed in many types of tissues, including the liver, lung, placenta, and brain, and was proved to be an identical protein to α2-macroglobulin receptor.[4,11] The gene coding for LRP1, located on chromosome 12 in segment q13-14, covers approximately 92 kb and includes 89 exons varying in size from 65 to 925 bases.[4,12,13]

2. Expression of LRP1 clusters II and IV in *Escherichia coli*

LRP1 contributes to a variety of physiological functions with its ligand binding. Therefore, it is essential to study the ligand binding of LRP1, especially on clusters II and IV, in research on the multifunctional nature of LRP1. For this, the production of recombinant LRP1 clusters II and IV

and their genetic modifications are indispensable to research on the function and interaction with the ligands of LRP1.[3,7]

Microbial systems can be an attractive platform to product recombinant proteins because of their high output without the cultivation of large weights or volumes. Among them, the *Escherichia coli* system is the most popular expression tool due to its inexpensive, fast, and high-density cultivation, relative simplicity, well-known genetics, and a number of compatible tools, such as various plasmids.[14,15,16] It seems like *E. coli* expression systems may be effective means for the production of recombinant LRP1, regardless to whether it is wild type or genetically modified, which is needed for various applications and research. Until now, however, the production of recombinant LRP1 or its fragments has been dependent on animal cells or the other microbial expression system in a number of previous studies.[7,17,18,19,20] In addition, for LRP1 fragments expressed with the *E. coli* expression system, just their binding properties have usually been focused on with ligands and crystallization for determining structures.[21,22,23] Therefore, we express LRP1 clusters II and IV, which play a leading role in the ligand binding of LRP1 in the *E. coli* system, purify them, and conduct a variety of experiments to prove their functionality by both biophysical and biochemical methods.

3. Coagulation factor VIII (fVIII)

The hemostatic system maintains a certain amount of blood in a fluid state under normal conditions and stops bleeding if a vessel injury occurs by forming a blood clot. The coagulation factor VIII (fVIII) is a proteinase that is associated with this hemostasis, and its deficiency results in hemophilia A.[24]

fVIII precursor is processed into a heterodimer with a heavy chain of 200 kDa containing the A1, A2, and B domains and a light chain of 80 kDa containing the A3, C1, and C2 domains and linked with a metal ion to the heavy chain. fVIII is activated with the cleavage of the B domain by thrombin, the activated fVIII (fVIIIa, Figure 2) forms complex fIXa, and the complex activates fX.[25,26,27]

FVIII is usually found in plasma. In the circulation, fVIII binds to various proteins; some participate in blood clotting, some behave as physiologic chaperones, and others are involved in the elimination of biologic wastes. The clearance of fVIII is conducted by endocytosis, and this process is usually mediated by LRP1.[28]

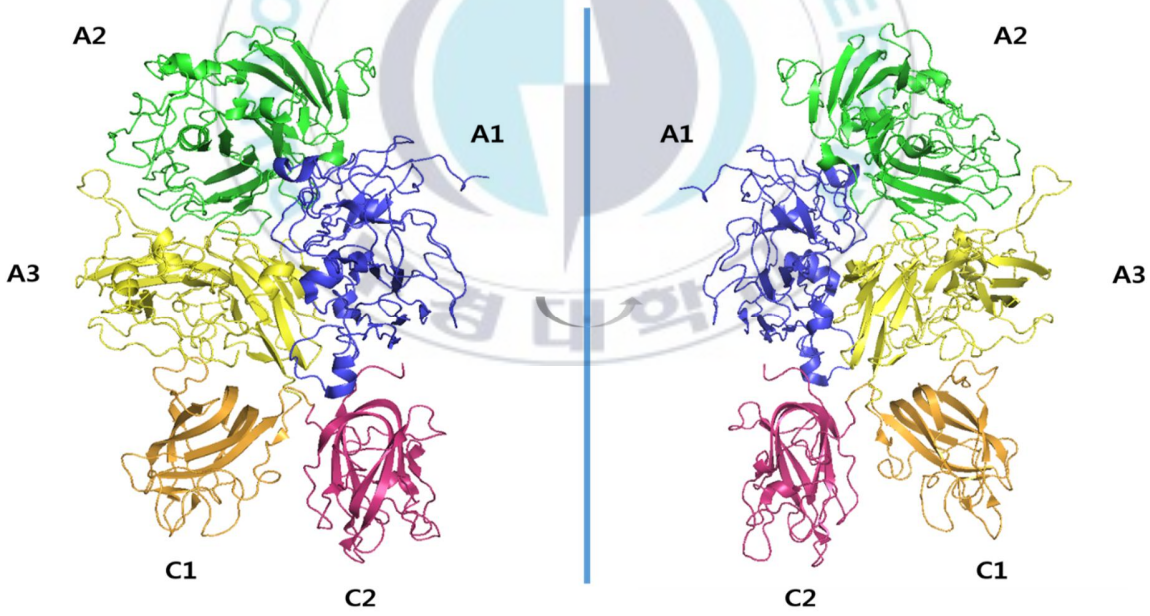

Figure 2. Crystal structure of B domain-deleted fVIII. A1 and A2 domains are in heavy chain, and C1, C2, and A3 domains are in light chain. PDB file is from Jacky Chi Ki Ngo et al.[29]

4. Receptor-associated protein (RAP)

RAP is an endoplasmic reticulum (ER) resident chaperone that plays a role in the proper maturation of several LDLR family members, such as LRP1. As a chaperone, RAP binds to LDLR family members with high affinity and prevents premature interaction between these proteins and their ligands in the ER. It protects receptors from lysosomal degradation and facilitates their delivery to the cell surface.[30,31,32,33,34,35]

This 39-kDa protein has three domains: D1, D2, and D3 (Figure 3). The D1 and D2 domains of RAP are involved in blocking the early interactions between LDLR family members and their ligands in the ER, and D3 domain is associated with the folding and trafficking of these proteins.[6,30,36]

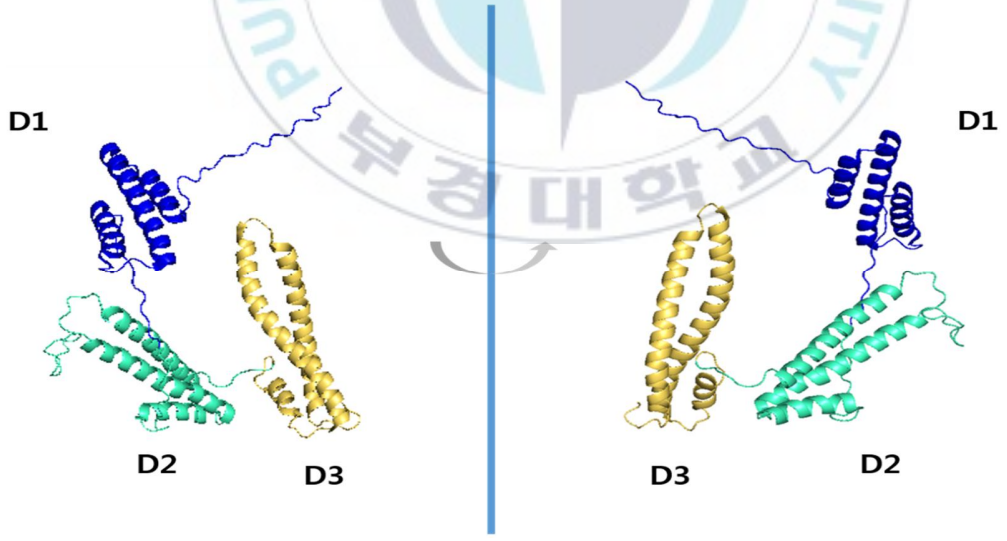

Figure 3. Structure of RAP determined with small-angle neutron scattering (SANS). PDB file is from Donghan Lee et al.[30]

In the binding of RAP to LDLR proteins, a model called the 'acidic necklace' was proposed by Carl Fisher et al.[37] In this model, bindings occur in the presence of calcium ion, and the binding site looks like a Ca^{2+}-centered cage. Carboxylate oxygen atoms from three aspartate residues on LDLR are coordinated with the center calcium ion and the surrounding 3-amino group of the lysine residue on RAP in a tripartite salt bridge.[37,17]

5. Surface plasmon resonance (SPR)

SPR is an electronic charge-density oscillation in the surface of metal thin film, and the resulting wave, a surface plasmon wave, proceeds along the boundary surface between the metal and dielectric materials. When the wavenumber vectors of the incident light and surface plasmon correspond with each other, the incident light excites the oscillation of surface electrons, and as a result, the light reflectance decreases. This is called attenuated total reflection. The incident angle with attenuated total reflection is a resonance angle, changing according to the weight of a medium with a relatively low refractive index. Using these principles, it is possible to obtain information about the protein–protein binding state from the change in the resonance angle.[38]

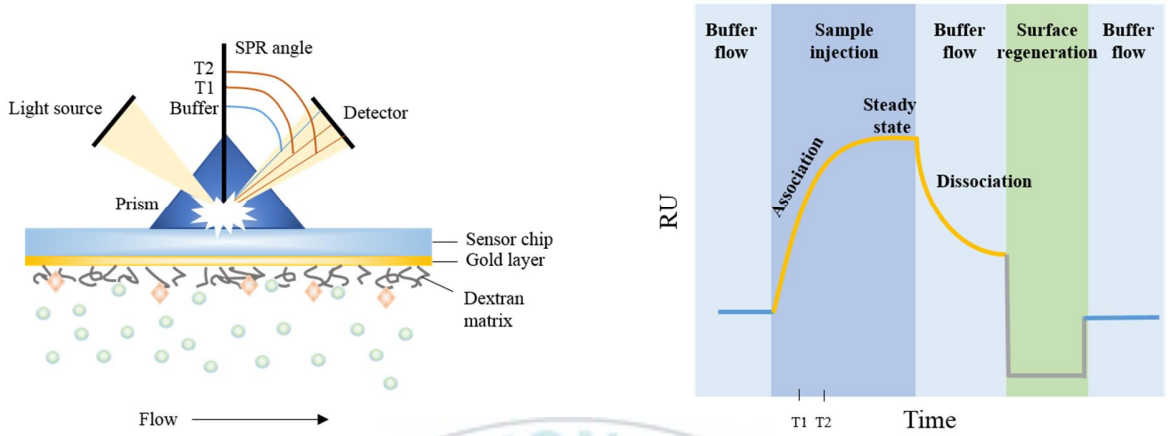

Figure 4. Mimetic diagram (left) and sensorgram (right) of SPR[39]

II. Materials and Methods

1. Cloning, expression, and purification of LRP1 clusters II and IV

The genes encoding LRP1 clusters II and IV, cloned in the pMT/Bip/V5-His vector, were gifts from Dr. Tongpil Min. The restriction enzyme sites of BamHI and XhoI were inserted into the genes by PCR using the i-Taq pre-mix (Intron, Korea). The details of the primer sequences of LRP1 clusters II and IV are listed in Table 2. The PCR products were purified with a DNA purification kit (Intron, Korea), digested with BamHI and XhoI enzymes (Takara Bio, Japan), and ligated with the pET His6 Sumo TEV LIC cloning vector (1S) (pETSUMO, a gift from Scott Gradia, Addgene plasmid #29659) using T4 DNA ligase (Takara Bio, Japan).

The recombinant vectors were introduced into *Escherichia coli* BL21(DE3), which were grown at

37 ˚C in LB medium containing 50 mg/L kanamycin until the absorbance of the culture at 600 nm reached 0.6. Protein overexpression was induced by the addition of isopropyl-β-D-1-thiogalactopyranoside (IPTG) up to a concentration of 0.5 mM. After 16 h of incubation at 20 ˚C, the cells were harvested by centrifugation for 30 min at 10,000 x g.

The cells were resuspended in 20-ml binding buffer (20-mM Tris-HCl, pH 7.5, 500-mM NaCl, 10-mM imidazole, 0.5-mM β-mercaptoethanol, 1mM-$CaCl_2$) per gram of pellet and sonicated on ice for 4 min followed by centrifugation for 30 min at 20,000 g. The recombinant proteins in the supernatant were bound to an Ni-NTA resin (ELPIS BIOTECH, Korea); pre-equilibrated with the binding buffer; washed with the buffer containing 20-mM Tris-HCl, pH 7.5, 500-mM NaCl, 50-mM imidazole, 0.5-mM β-mercaptoethanol, and 1-mM $CaCl_2$; and eluted with the buffer containing 20-mM Tris-HCl, pH 7.5, 500-mM NaCl, 250-mM imidazole, 0.5-mM β-mercaptoethanol, and 1-mM$CaCl_2$. Ubiquitin-like-specific protease 1 (Ulp-1) was added to the purified SUMO-fusion protein for the cleavage of His6-tag as well as SUMO-tag. After 4.5 h of incubation at RT, tag-cleaved proteins underwent size exclusion chromatography with buffer A (20-mM Tris-HCl, pH 7.5, 150-mM NaCl, 1-mM $CaCl_2$). The homogenous fractions were concentrated to 4 mg/mL using a 10-kDa cut-off membrane filter and centrifugation at 3000 x g.

Table 2. The sequences of primers used to introduce restriction enzyme sites (underlying) to the genes encoding LRP1 clusters II and IV.

Primer	Sequences
LRP1 cluster II forward primer	ATTATGGATCCGTGCCTCCACCCCAGT
LRP1 cluster II reverse primer	ATTCTCGAGTCACTGGTCGCAGAGCTC
LRP1 cluster IV forward primer	ATTGGATCCTGTGTGTCCAACTGCAC
LRP1 cluster IV reverse primer	ACTCTCGAGTCATCAGCTTGGGGTCGAT

2. Cloning, expression, and purification of RAP

The gene of RAP was synthesized and cloned in pGEX-4T-2, and GST (Glutathione transferase)–fusion RAP was expressed in BL21(DE3) cells. The cells were grown to OD_{600} = 0.5 in LB medium containing 0.5-mg/L ampicillin, induced with 0.5-mM IPTG and harvested after 5 h of incubation at 25 ˚C.

The cells were resuspended in 10-ml binding buffer (20-mM potassium phosphate buffer, pH 7.0, 0.1-mM EDTA) per gram of pellet and sonicated on ice for 4 min followed by centrifugation for 15 min at 20,000 xg and collection of the supernatant. The GST-fusion protein was bound to a GST-bind agarose resin (Elpis Biotech, Korea) pre-equilibrated with the binding buffer. Column washing was conducted with 10 column volumes of binding buffer, and protein bound to resin was eluted with the elution buffer (Tris-HCl 50 mM, pH 8.0, 15-mM reduced glutathione, 150-mM NaCl). GST-tag was not cleaved since it does not interfere with binding to LRP1.[40] Therefore, GST-RAP protein after a buffer change to buffer B (10-mM HEPES, pH 7.5, 0.005% Tween20, 5-mM $CaCl_2$, 150-mM NaCl) was used in the experiments. It was concentrated to 1 mg/mL using a 10-kDa cut-off membrane filter and centrifugation at 3000 x g.

3. Preparation of fVIII

Coagulation factor VIII was a gift from Green Cross (Korea). It was dissolved to 0.1 mg/mL in buffer B.

4. Characterization of LRP1 clusters II and IV

4.1. Analytical size exclusion chromatography (ASEC)

The molecular weights of LRP1 clusters II and IV were determined by gel filtration on a Superdex 200 10/300 GL column (GE Healthcare, USA) pre-equilibrated in buffer A. For a particular molecule, its elution was described in terms of the corresponding K_{av} value: $K_{av}=(V_e-V_o)/(V_t-V_o)$, where V_e is the elution volume for the particular protein, V_o is the void volume, and V_t is the total bed volume of the column. V_o was measured as 9.385 mL with Blue Dextran (Sigma-Aldrich, USA), and V_t of the column was 24 mL. The column was calibrated with a mixture of cytochrome C (12.4 kDa), carbonic anhydrase (29 kDa), bovine serum albumin (66 kDa), and β-amylase (200 kDa). The concentrations of purified LRP1 clusters II and IV were 1.17 mg/mL and 1.10 mg/mL, respectively, in buffer A with and without 1-mM dithiothreitol (DTT), and the proteins were passed into the column at a flow rate of 1 mL/min.

4.2. Analytical ultracentrifugation (AUC)

Sedimentation velocity experiments were performed using a ProteomeLab XL-A analytical ultracentrifuge (Beckman Coulter, Inc., USA). Purified LRP1 clusters II and IV were analyzed in buffer A at concentrations of 0.4 mg/mL and 0.45 mg/mL, respectively, and their stability in 20 ℃ for 9 h was confirmed using SDS-PAGE before ultracentrifugation. Data was collected at 40,000 rpm at 20 °C by measuring the absorbance at 280 nm. Data collected every 3 min for 9 h was analyzed with the SEDFIT Version 144d program, and the partial specific volume of the proteins and the density of the solvent were calculated using Sednterp software.

4.3. Circular dichroism (CD) spectroscopy

CD spectra were recorded by a Chirascan CD spectrometer (Applied Photophysics, US) at 20 ˚C using a quartz cuvette (Hellma Inc., Germany) with 1-mm path length with a PTFE stopper. Scans

were performed from 190 to 260 nm, repeated five times, and averaged. LRP1 clusters II and IV in buffer A were diluted to 0.5 mg/mL with or without Ethylene glycol-bis(2-aminoethylether)-N,N,N′,N′-tetraacetic acid (EGTA), respectively. Before the experiments, 0.1-mM EGTA was added to protein samples with EGTA and the samples were given 30 min for reaction at RT.

4.4. Fluorescence emission spectroscopy

Emission fluorescence spectra were recorded on a FP-6300 spectrofluorometer (Jasco, Japan) from 300 to 500 nm at 20 ℃ with excitation at 280 nm. LRP1 clusters II and IV in buffer A were diluted to 0.2 and 0.3 mg/mL, respectively, and 1-mM DTT, 6-M urea, and 0.1-mM EGTA were added to the samples.

4.5. Interaction of LRP1 clusters II and IV

Purified LRP1 clusters II and IV in buffer A changed the buffer to buffer B through gel filtration with a HiLoad 16/600 Superdex 200-pg size-exclusion column. Then, they were concentrated to 10 μM using a 10-kDa cut-off membrane filter and centrifugation at 3000 xg. Subsequently, they were additionally diluted to 7.5, 5, 2.5, 1, and 0.5 μM. The concentrations of RAP and fVIII were set to 0.3 mM in buffer B.

SPR was performed using an SR7500DC SPR system (Reichert Technology, USA). After the ligands were immobilized to the gold-PEG chip (Reichert Technology, USA) by flowing them for 10 min at a rate of 20 μL/min, LRP1 cluster II or IV in buffer B was applied at a flow rate of 30 μL/min for 3 min and dissociation was measured by flowing buffer B over the chip for 7 min at a flow rate of 30 μL/min. Data was analyzed with Scrubber 2 software.

III. Results

1. Cloning, expression, and purification of LRP1 clusters II and IV

By PCR, genes encoding LRP1 clusters II and IV were amplified and their sizes, 1010 bp (cluster II) and 1360 bp (cluster IV), were verified by agarose gel electrophoresis (Figure 5). The maps of the recombinant pETSUMO vectors are shown in Figures 6 and 7, and the sequences inserted into them were proved to correspond with the LRP1 gene sequences (Figure 8) by a gene sequencing service (Macrogen, Korea). To express two recombinant proteins, the vectors were transformed into BL21(DE3) by the heat-shock method. Figure 9 shows that LRP1 clusters II (36.7 kDa) and IV (50.8 kDa) were overexpressed in soluble form. SUMO-tag, in fact 12 kDa, appeared to be ~20 kDa in SDS-PAGE gel. Therefore, the recombinant proteins had their bands at ~56 kDa and ~70 kDa with SUMO-tag. After SUMO-tag cutting by Ulp-1 overnight, SUMO-tag was separated from the target proteins using gel filtration, as shown in Figure 10. SDS-PAGE analysis revealed that oligomerization occurred and dramatically decreased the final protein yield, since only homogenous fractions were collected. The final protein productions of LRP1 clusters II and IV were approximately 1.6 mg (cluster II) and 1 mg (cluster IV) per liter of LB medium.

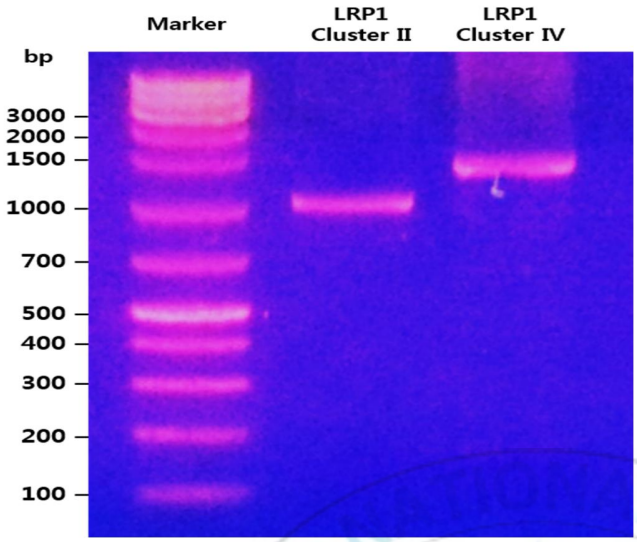

Figure 5. PCR products of LRP1 clusters II and IV

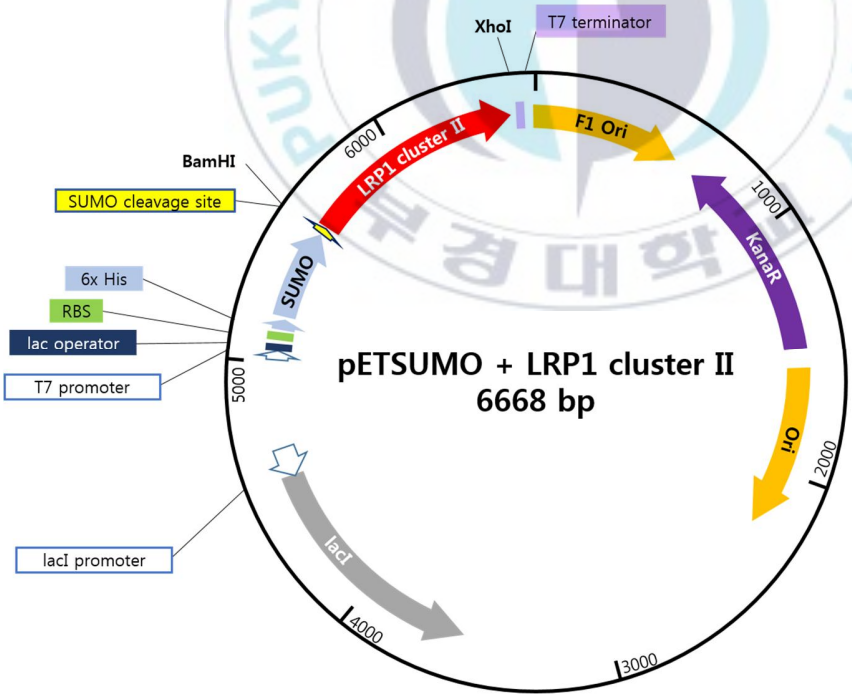

Figure 6. Recombinant pETSUMO with LRP1 cluster II gene

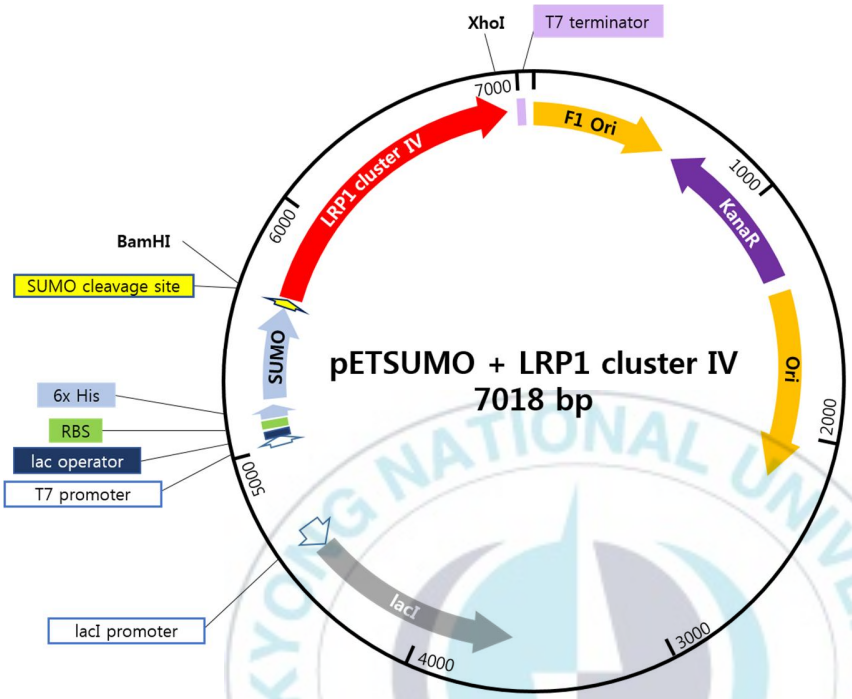

Figure 7. Recombinant pETSUMO with LRP1 cluster IV gene

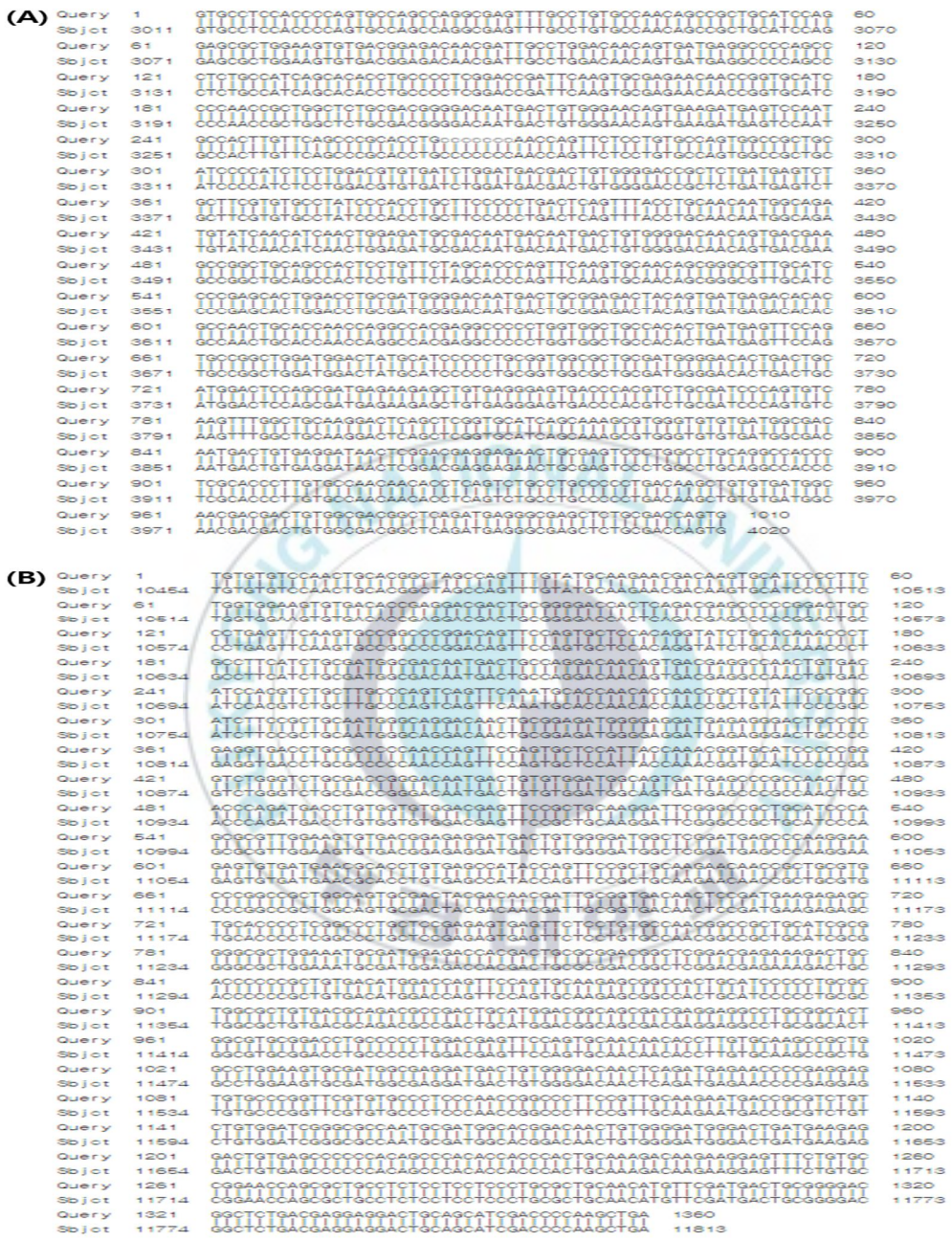

Figure 8. Sequencing of recombinant vector with LRP1 clusters II (A) and IV (B). "Query" lines indicate the sequences of recombinant plasmid identified by gene sequencing (Bioneer, Korea), and "sbjct" lines are LRP1 mRNA sequences from sequence ID NM_002332.2.

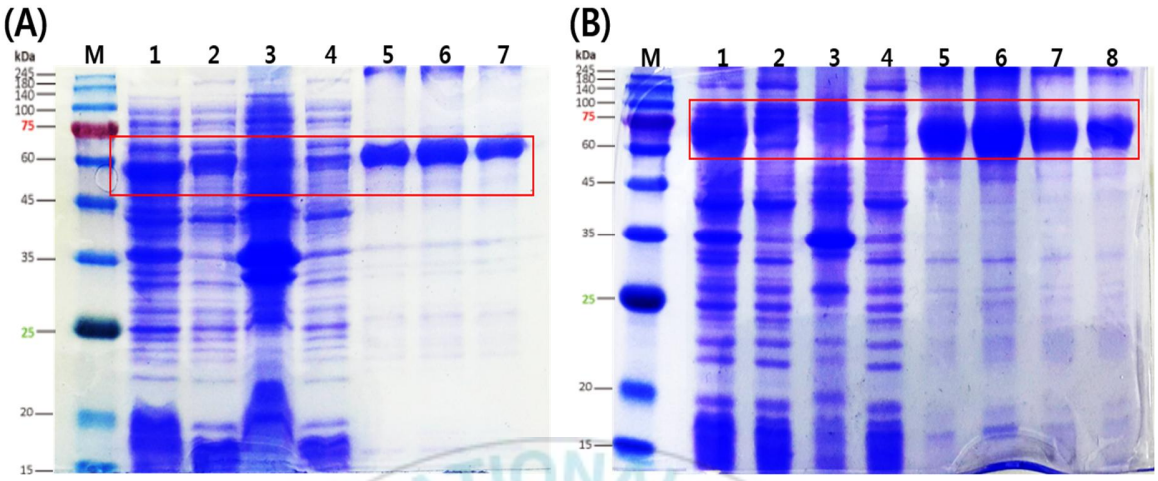

Figure 9. Expression and purification of LRP1 clusters II (A) and IV (B). 1, lysate; 2, supernatant; 3, pellet; 4, flow-through; 5-8, elution

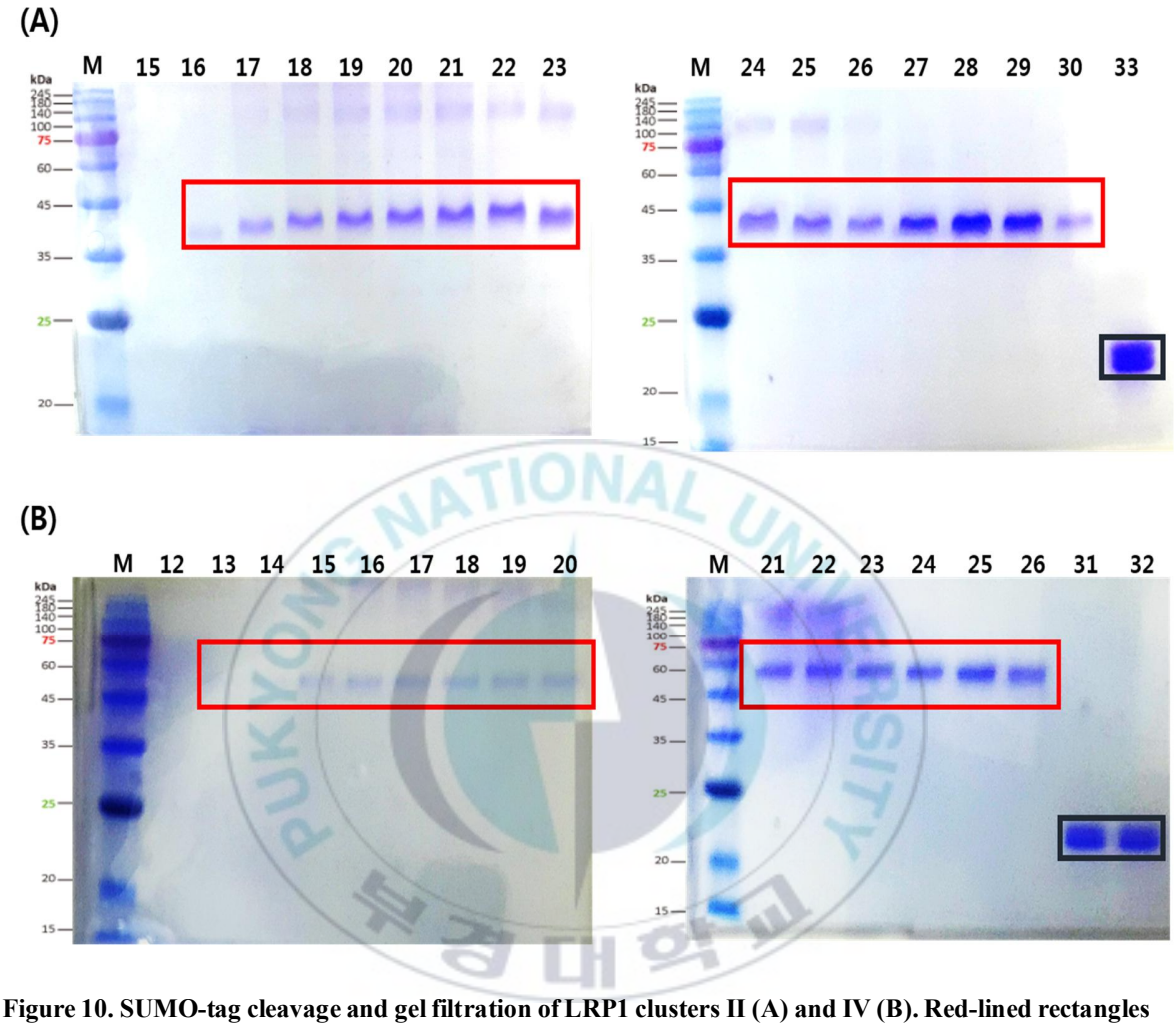

Figure 10. SUMO-tag cleavage and gel filtration of LRP1 clusters II (A) and IV (B). Red-lined rectangles are target protein without SUMO-tag, and black-lined rectangles are SUMO-tag and amino acid sequences before it, including His-tag.

2. Cloning, expression, and purification of RAP

The RAP gene was synthesized and cloned in pGEX-4T-2 with gene synthesis and the cloning service (Bioneer, Korea) (Figure 11).

The vectors transformed into BL21(DE3) expressed RAP in soluble form, as shown in Figure 12. GST-tag was approximately 25 kDa; thus, the recombinant protein had its bands at approximately 60 kDa with GST-tag. Since most GST-RAP proteins remained in the flow-through, as shown in Figure 12, the flow-through was recycled to purify GST-RAP three times. As a result, the final protein production of RAP was approximately 6 mg per liter of LB medium.

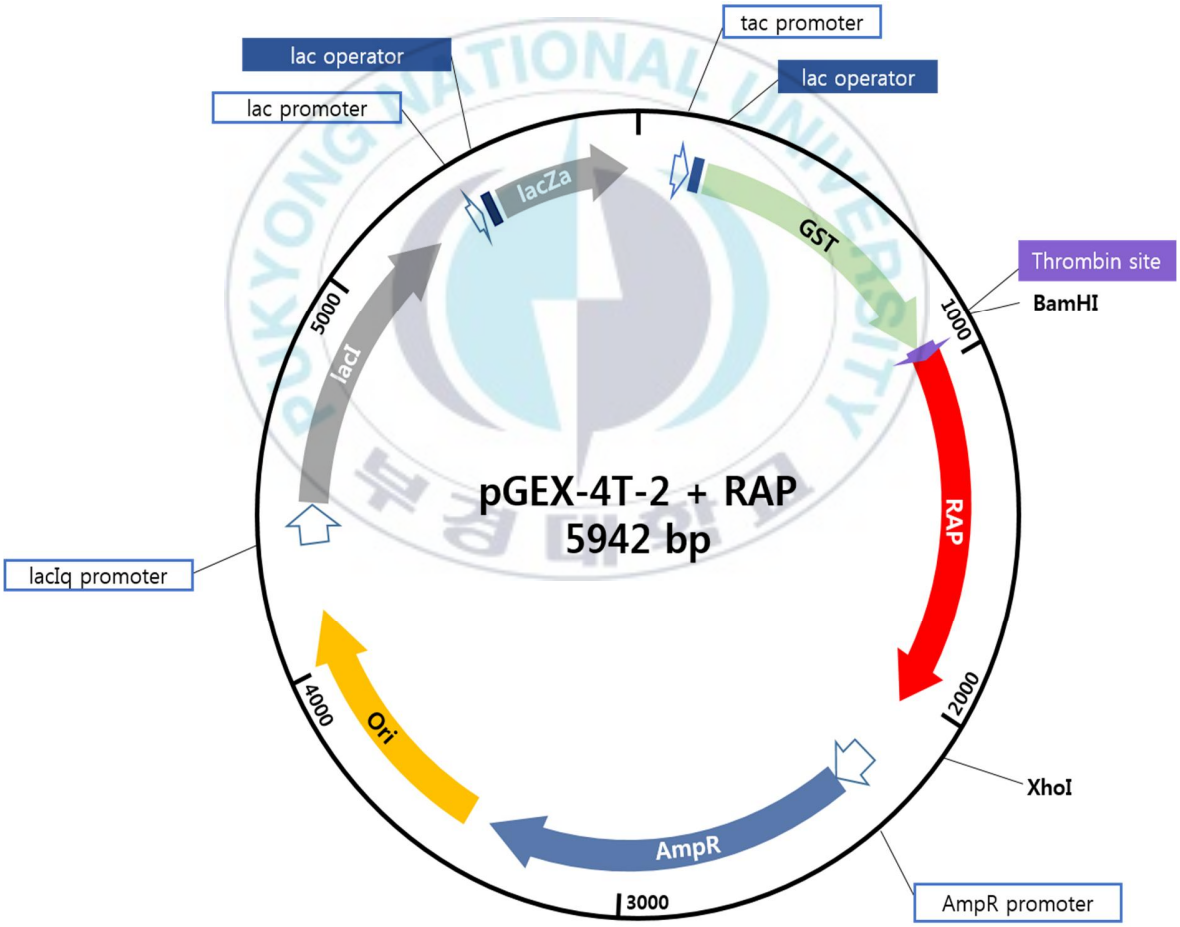

Figure 11. Recombinant pGEX-4T-2 with RAP gene

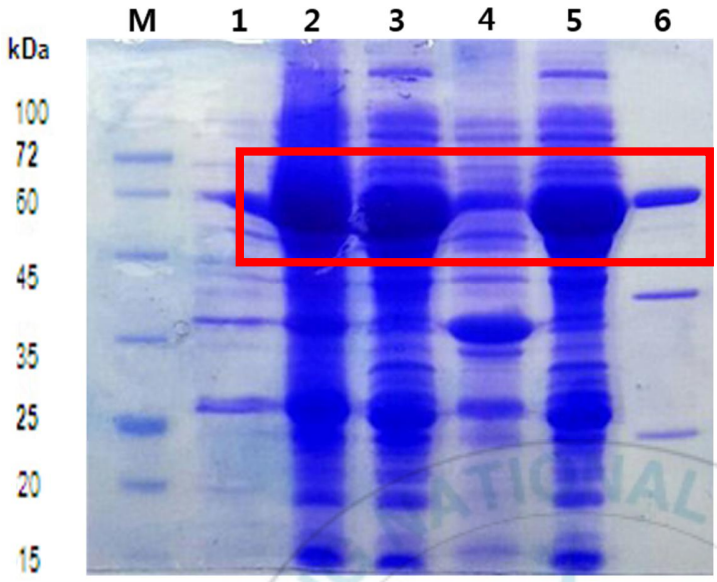

Figure 12. Expression and purification of RAP. 1, Uninduced cell; 2, lysate; 3, supernatant; 4, pellet; 5, flow-through; 6, elution. The red-lined rectangle shows RAP-GST recombinant protein.

3. ASEC

The partition coefficient (K_{av}) is described by the equation below, and the logarithm of the molecular weight can be plotted as the linear function of K_{av}. The linear equation of the calibration curve from the chromatogram of the protein marker was y = -3.076x + 3.0691 (Figure 13B).[41,42]

As shown in Figure 13, the ASEC chromatograms show that LRP1 clusters II and IV had two peaks, regardless of whether 1-mM DTT was present. In all chromatograms, the molecular weights calculated from the first peaks were approximately double those calculated from the second peaks. If monomers appeared to be the second peaks, the first peaks indicated the existence of dimers. However, in comparison to the actual molecular weights of the LRP1 cluster II and IV monomers, the molecular

weights from the second peaks had high values (Figure 13 and Table 3), which seems to be due to their shape.

4. AUC

The sedimentation coefficient of a macromolecule (s) is given by the Svedberg equation below.[43]

$$s = \frac{u}{\omega^2 r} = \frac{M(1 - V_{bar}\rho)}{N_A f} = \frac{MD(1 - V_{bar}\rho)}{RT}$$

(u, the observed radial velocity of protein; ω, the angular velocity of the rotor; r, the radial position; $\omega^2 r$, the centrifugal field; M, the molar mass; v, the partial specific volume; ρ, the density of the solvent; N_A, Avogadro's number; f, the frictional coefficient; D, the diffusion coefficient; and R, the gas constant)

The ratio of the maximum s-value to the observed s-value is equal to the ratio of the experimental frictional coefficient to the minimum frictional coefficient, which measures the maximum shape asymmetry from a sphere.[43] This ratio of LRP1 clusters II and IV was 1.40998 and 1.26419, respectively. The molecular weight distribution showed relatively similar molecular weights to the actual values and the existence of dimers, as in the ASEC experiments (Figures 13 and 14). Considering the frictional ratio of LRP1 cluster II was larger than that of cluster IV, it is consistent that the estimated molecular weight of cluster IV was more similar to the actual value than the estimated size of cluster II. This difference may have resulted from both geometrical shape asymmetry and hydration expansion.

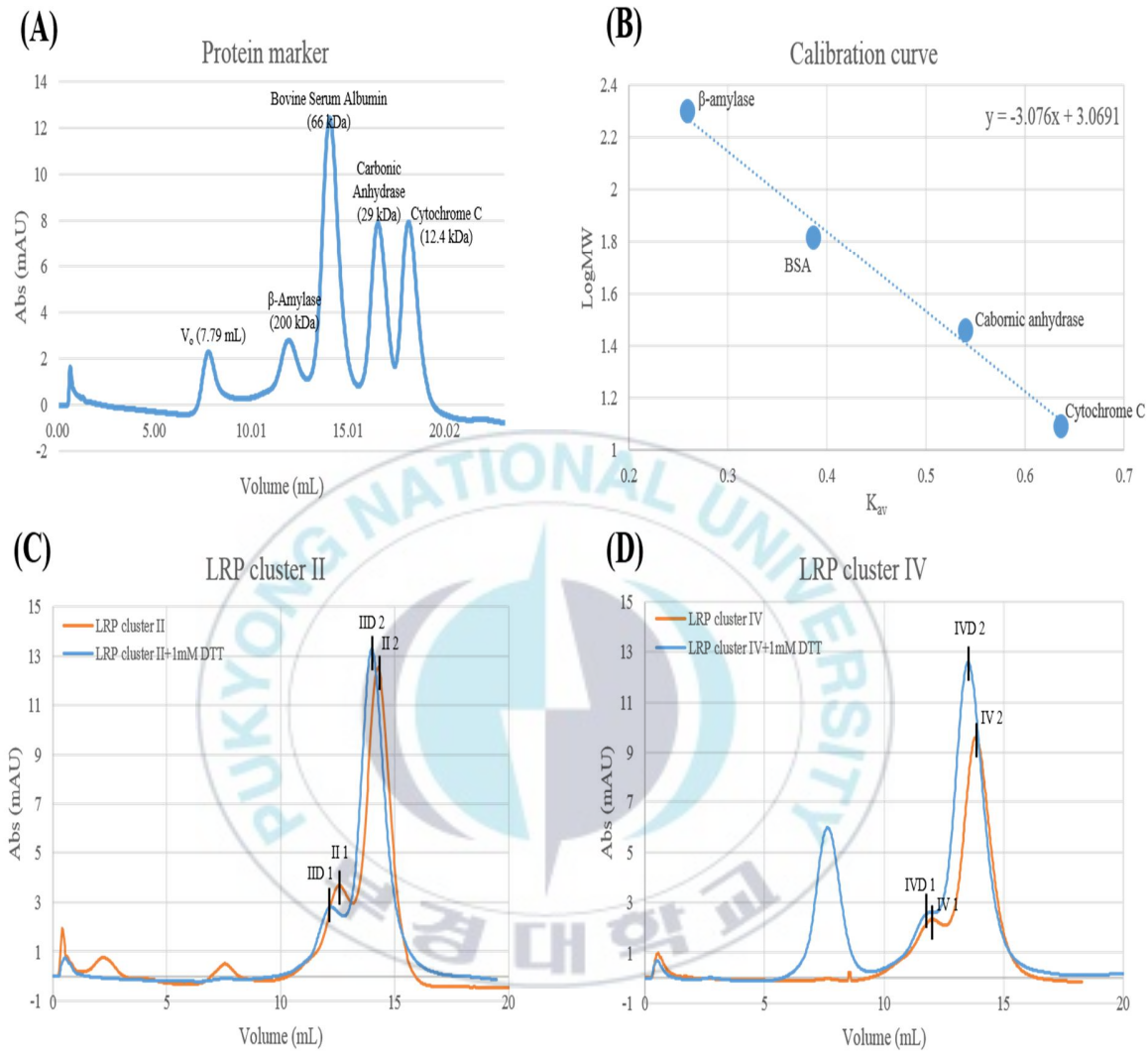

Figure 13. ASEC chromatogram of protein marker (A), LRP1 cluster II (C), cluster IV (D). (B) is calibration curve from (A).

Table 3. Molecular weights calculated from ASEC chromatogram and calibration curve.

Peak	Volume (mL)	Kav	log MW	MW (kDa)
II 1	12.692	0.302406	2.138899	137.689044
II 2	14.184	0.394448	1.855778	71.742804
IID1	12.292	0.27773	2.214803	163.984631
IID2	14.101	0.389328	1.871528	74.3923671
IV 1	12.04	0.262184	2.262623	183.072249
IV 2	13.951	0.380074	1.899992	79.4314131
IVD 1	11.827	0.249044	2.303041	200.928374
IVD 2	13.441	0.348612	1.99677	99.2589294

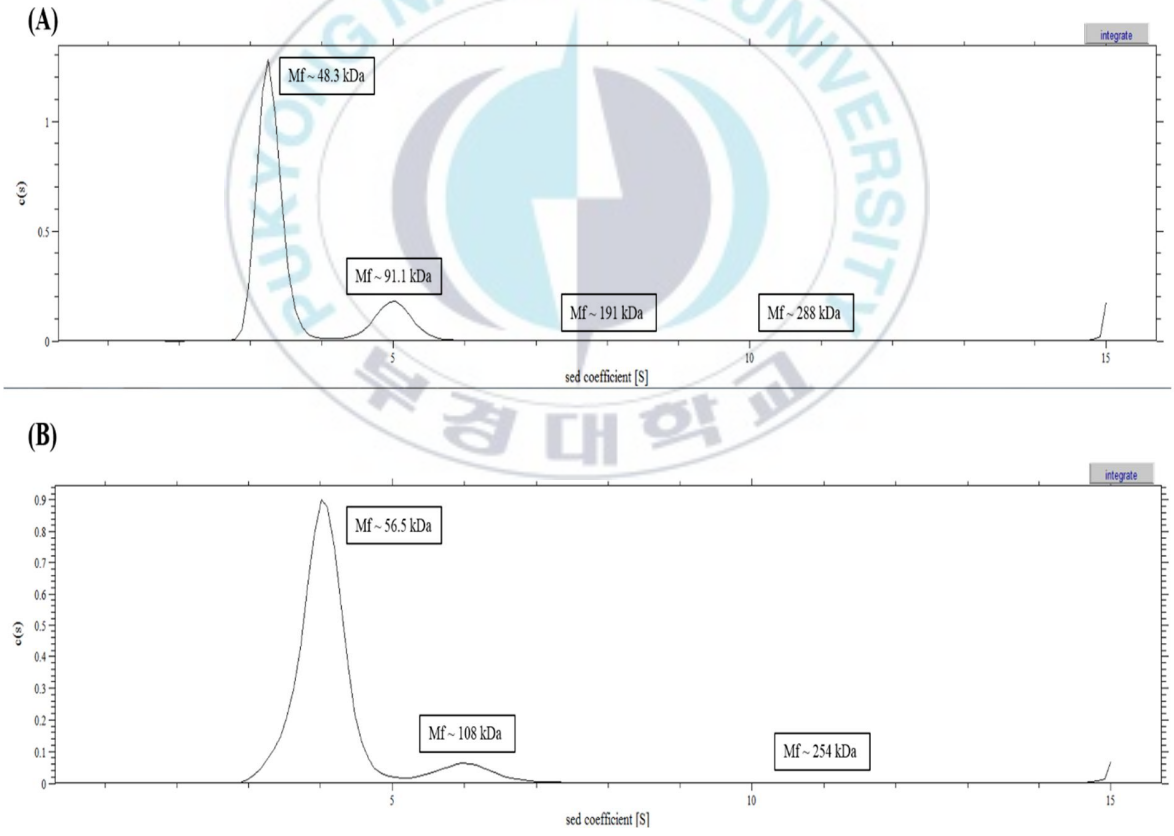

Figure 14. Molecular weight distribution of LRP1 clusters II (A) and IV (B) determined from AUC

5. Fluorescence emission spectroscopy

Fluorescence emission spectroscopy was conducted to determine the folding state change of LRP1 clusters II and IV with 1-mM DTT, 6-M urea, and 0.1-mM EGTA. In the spectrum of LRP1 cluster II, the samples with the addition of urea decreased the fluorescence signal, which means a partial change of the folding state, and samples with EGTA showed a completely unfolded state with a slight signal, while samples with DTT emitted an increased signal to samples with no reagent (Figure 15). The effect of EGTA was similar in the LRP1 cluster IV sample. This means that EGTA, a Ca^{2+} scavenger, directly affected the fluorescence emission of LRP1 clusters II and IV and Ca^{2+} ion had a critical impact on their tertiary structure. Additionally, in LRP1 cluster IV samples, a slight fluorescence shift was observed, while the intensities of the signals were relatively constant.

6. CD spectroscopy

CD spectroscopy experiments for a wavelength of 200–260 nm were also conducted for obtaining information about the second structure of the recombinant proteins. The spectra of the protein samples with/without EGTA appeared to be similar, and the calculated second-structure compositions through http://cbdm-01.zdv.uni-mainz.de/~andrade/k2d2/index.html were completely the same with 84.27% α-helix and 1.24% β-sheet in all protein samples. The predicted spectrum according to this composition was totally different from the actual CD spectra, which means that the secondary-structure compositions predicted from these spectra were not reliable (Figures 16 and 17).

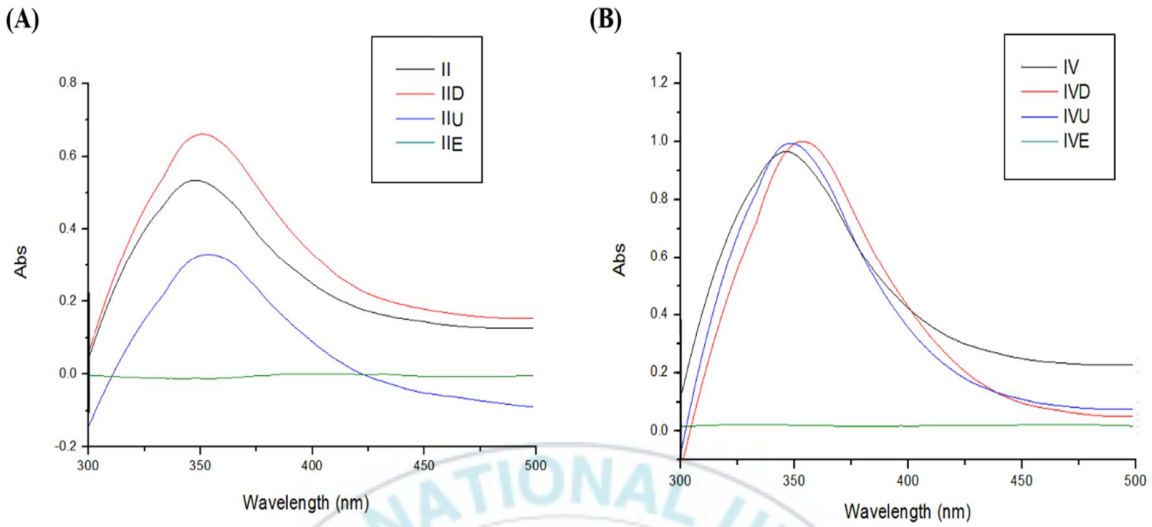

Figure 15. Fluorescence emission spectra of LRP1 clusters II (A) and IV (B). II, LRP1 cluster II; IV, LRP1 cluster IV; D, adding 1-mM DTT; U, adding 6-M urea; E, adding 0.1-mM EGTA

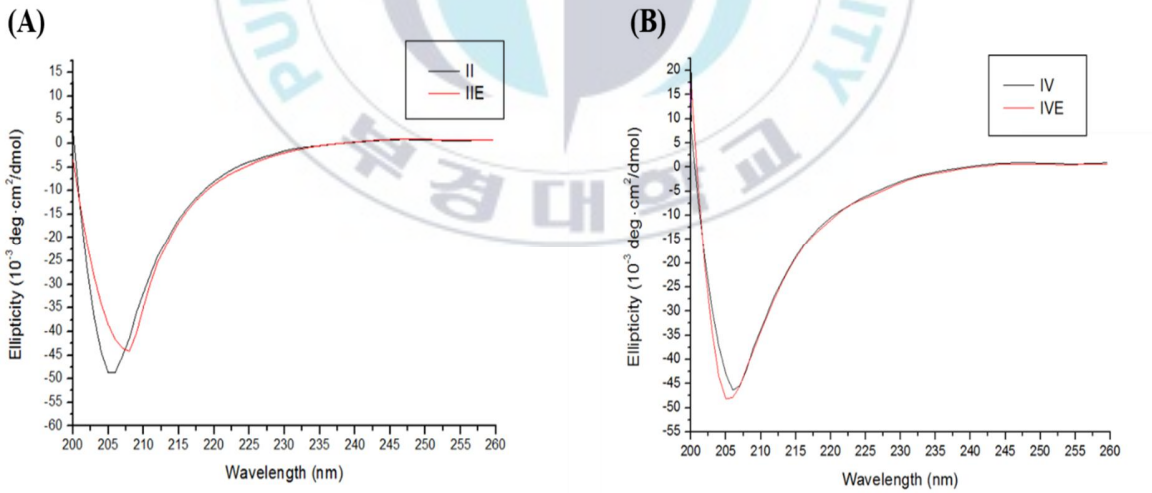

Figure 16. CD spectra of LRP1 clusters II (A) and IV (B). II, LRP1 cluster II; IV, LRP1 cluster IV; E, adding 0.1-mM EGTA

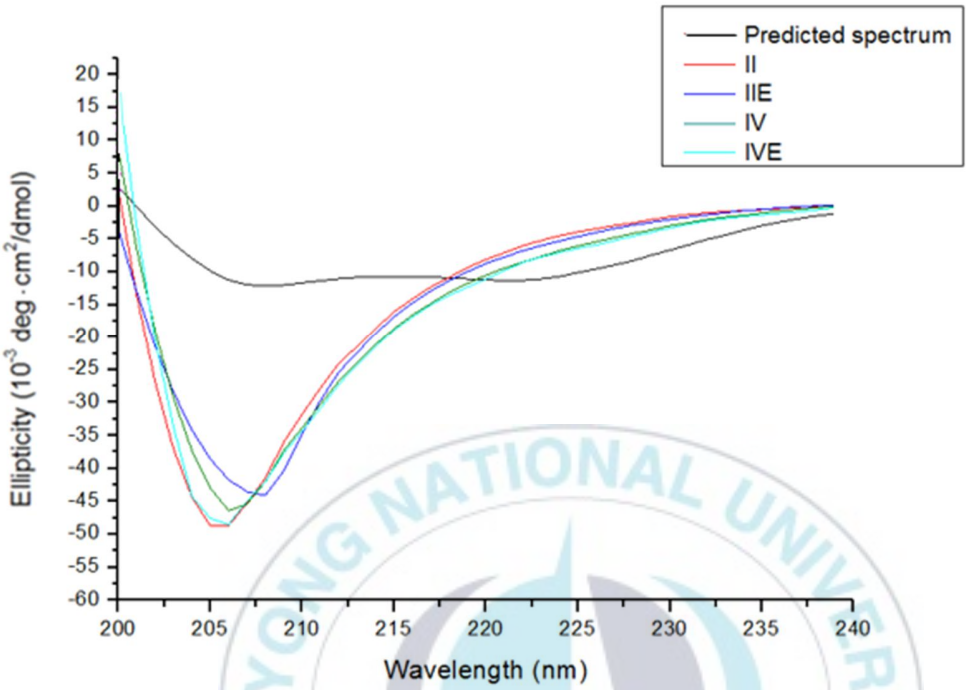

Figure 17. CD spectra of samples and predicted spectrum from calculated secondary-structure composition. II, LRP1 cluster II; IV, LRP1 cluster IV; E, adding 0.1-mM. EGTA max error was too large (approximately 0.4) according to calculation in http://cbdm-01.zdv.uni-mainz.de/~andrade/k2d2/index.html

7. SPR

The affinity between two proteins can be determined with the dissociation constant (K_D) using SPR analysis. The interactions of LRP1 clusters with two ligands (RAP and fVIII) were observed by SPR experiments. For SPR, the K_D values are shown in Table 4. The affinity of LRP1 cluster II to RAP was much higher than that of cluster IV, and for fVIII, the affinity of cluster II was higher than that of cluster IV, also. Overall, recombinant proteins have low affinity to their ligands except

the affinity of cluster II to RAP.

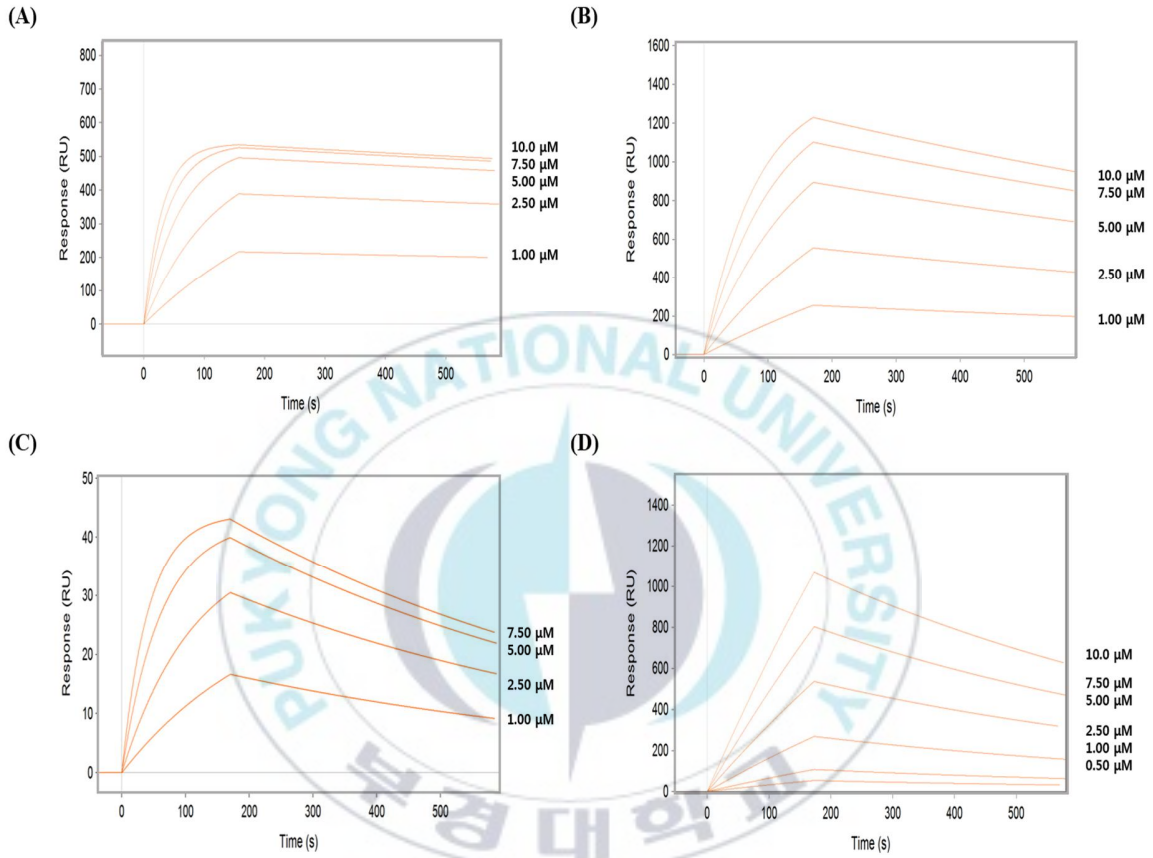

Figure 18. SPR analysis of the interaction between recombinant LRP1 fragments and their ligands. (A) The interaction between RAP and LRP1 cluster II. (B) The interaction between RAP and LRP1 cluster IV. (C) The interaction between fVIII and LRP1 cluster II. (D) The interaction between fVIII and LRP1 cluster IV.

Table 4. K_D values in the interactions of LRP1 clusters and their ligands, RAP and fVIII

	LRP1 cluster II	LRP1 cluster IV
RAP	57 nM	530 nM
fVIII	482 nM	780 nM

IV. Discussion

LRP1 is a multifunctional receptor associated with various biological processes through binding with dozens of ligands. For medical and industrial applications, there are a number of advantages to expressing it as a recombinant protein in *E. coli* due to its low cost and space for cultivation. Therefore, I expressed LRP1 clusters II and IV, which mainly contribute to ligand binding, in *E. coli* and conducted biophysical and biochemical analyses to study the properties of the recombinant proteins. Through this, this research aims to find the availability of recombinant LRP1 or its fragments expressed in *E. coli* and provide information for related studies.

LRP1 clusters II and IV inserted into a pETSUMO vector were expressed in BL21(DE3). The recombinant proteins were proved to be soluble and overexpressed through SDS-PAGE. However, their final yield was relatively low because of the formation of oligomers in the gel filtration step after SUMO-tag cleavage using Ulp-1. Additionally, in the AUC and ASEC experiments, the samples from the homogenous monomer fraction showed dimerization and trimerization. This oligomerization is widely shown in LRP1 regardless of the expression hosts and whether the protein is from nature or recombinant.[44,45,46] In addition, the molecular weights of the recombinant protein monomers calculated from the AUC and ASEC data were higher than their actual values, which

shows the effect of geometrical shape asymmetry and hydration expansion.

Fluorescence emission spectra were recorded from 300–500 nm with an exciting wavelength of 280 nm. With 0.1-mM EGTA, both LRP1 clusters II and IV showed no fluorescence signal. This suggests that the Ca^{2+} ion, which is reported to be important for the ligand binding of clusters II and IV,[23,37,47] largely contributes to the folding of the recombinant proteins. Considering folding is much more complicated in eukaryotic cells than in prokaryotic ones, however, the weak tertiary structure of EGTA may have resulted from expression in *E. coli*. LRP1 cluster II samples with 6-M urea showed a decreased signal, while 1-mM DTT increased the fluorescence signal. The change in the fluorescence signal intensity came from the conformational change in the tryptophan and tyrosine residues located toward the core of protein in the native state. The more they are exposed to a hydrophilic environment, such as aqueous solvent, the less they can emit fluorescence. Thus, DTT may tend to locate tryptophan and tyrosine residues more toward the core of the proteins, while urea exposes them to aqueous solution by denaturing the proteins. Given that DTT may contribute to eliminating disulfide bonds on LRP1 clusters containing many cysteine side chains, their removal locates tryptophan and tyrosine residues toward the core.

CD experiments were conducted on recombinant LRP1 cluster II and IV samples with and without EGTA, and the secondary-structure compositions of the proteins were calculated from the CD results. The spectra of the protein samples with and without EGTA appeared to be similar, and the calculated second-structure compositions were also the same with 84.27% α-helix and 1.24% β-sheet in all protein samples. However, this is not a reliable result, as the max error reached 0.4 and the corresponding spectrum does not agree with the CD spectra from the experiments. The secondary structures of CR3, CR7, and CR8 in cluster II were determined with NMR spectroscopy

and X-ray crystallography. They usually had two antiparallel β-sheets and one or one and a quarter turns of α-helix and were all expressed in *E. coli*.[23,48,49] Considering this, the predicted second structures were not consistent with the real structure.

For the biochemical analysis of recombinant LRP1 clusters II and IV, SPR experiments were conducted with the ligands of fVIII and RAP. With two ligands, both RAP and fVIII, the K_D values of the two recombinant proteins were much higher than previously reported proteins expressed in animal cells (Table 5),[7] which means much lower affinities to ligands.

Table 5. K_D values in SPR analysis. K_D values of recombinant proteins expressed in animal cells are from J. G. Neels et al.[7] In SPR experiments with proteins expressed in animal cells, fVIII light chain was used instead of full-length fVIII.

	Expressed in *E. coli*		Expressed in animal cells	
	LRP1 cluster II	**LRP1 cluster IV**	**LRP1 cluster II**	**LRP1 cluster IV**
RAP	57 nM	530 nM	12. 7 nM	18 nM
fVIII	482 nM	780 nM	121.4 nM	87.8 nM

V. Conclusion

To test the properties of recombinant LRP1 clusters II and IV expressed in *E. coli*, a series of experiments were conducted. As a result, recombinant LRP1 clusters II and IV expressed with pETSUMO as a vector and BL21(DE3), a strain of *E. coli*, showed oligomerization, as observed in nature or recombinant LRP1 clusters expressed in animal cells. Their folding was weak to the Ca^{2+}

scavenger, EGTA, and their predicted secondary structures were not consistent with the actual structure of LRP1 clusters II and IV. The affinity of the proteins to two ligands, RAP and fVIII, was much lower than that of protein expressed in animal cells. However, it seems that additional experiments using other vectors, *E. coli* strains, and different conditions of induction are needed to ensure the difference in biophysical and biochemical properties according to the expression host.

VI. References

1. Willnow, T. E., Nykjaer, A. & Herz, J. Lipoprotein receptors: new roles for ancient proteins. *Nat. Cell Biol.* **1,** E157-62 (1999).
2. Herz, J. & Strickland, D. K. LRP: A multifunctional scavenger and signaling receptor. *J. Clin. Invest.* **108,** 779–784 (2001).
3. Lillis, A. P., Duyn, L. B. V. A. N., Murphy-ullrich, J. E. & Strickland, D. K. LDL Receptor-Related Protein 1 : Unique Tissue-Specific Functions Revealed by Selective Gene Knockout Studies. 887–918 (2008). doi:10.1152/physrev.00033.2007.
4. Neels, J. G., Horn, I., van den Berg, B. M. M., Pannekoek, H. & van Zonneveld, A.-J. Ligand-receptor interactions of the low density lipoprotein receptor- related protein , a multi-ligand endocytic receptor. *Fibrinolysis & Proteolysis* **12,** 219–240 (1998).
5. Neels, J. G., Bovenschen, N., Van Zonneveld, A. J. & Lenting, P. J. Interaction between Factor VIII and LDL receptor-related protein. Modulation of coagulation? *Trends Cardiovasc. Med.* **10,** 8–14 (2000).

6. Bu, G. & Schwartz, A. L. RAP a novel type of ER chaperone. *Trends Cell Biol.* **8,** 272–276 (1998).

7. Neels, J. G. *et al.* The second and fourth cluster of class A cysteine-rich repeats of the low density lipoprotein receptor-related protein share ligand-binding properties. *J. Biol. Chem.* **274,** 31305–31311 (1999).

8. Herz, J. *et al.* Surface location and high affinity for calcium of a 500-kd liver membrane protein closely related to the LDL-receptor suggest a physiological role as lipoprotein receptor. *EMBO J.* **7,** 4119–4127 (1988).

9. Rudenko, G. Structure of the LDL Receptor Extracellular Domain at Endosomal pH. *Science (80-.).* **298,** 2353–2358 (2002).

10. Gotthardt, M. *et al.* Interactions of the low density lipoprotein receptor gene family with cytosolic adaptor and scaffold proteins suggest diverse biological functions in cellular communication and signal transduction. *J. Biol. Chem.* **275,** 25616–25624 (2000).

11. Kristensen, T. *et al.* Evidence that the newly cloned low-density-lipoprotein receptor related protein (LRP) is the α2-macroglobulin receptor. *FEBS Lett.* **276,** 151–155 (1990).

12. Hilliker, C., Van Leuven, F. & Van Den Berghe, H. Assignment of the gene coding for the ??2-macroglobulin receptor to mouse chromosome 15 and to human chromosome 12q13-q14 by isotopic and nonisotopic in situ hybridization. *Genomics* **13,** 472–474 (1992).

13. Van Leuven, F. *et al.* Structure of the gene (LRP1) coding for the human alpha 2-macroglobulin receptor lipoprotein receptor-related protein. *Genomics* **24,** 78–89 (1994).

14. Rosano, G. L. & Ceccarelli, E. A. Recombinant protein expression in Escherichia coli: Advances and challenges. *Front. Microbiol.* **5,** 1–17 (2014).

15. Chen, R. Bacterial expression systems for recombinant protein production: E. coli and beyond. *Biotechnol. Adv.* **30,** 1102–1107 (2012).

16. Sørensen, H. P. & Mortensen, K. K. Advanced genetic strategies for recombinant protein expression in Escherichia coli. *J. Biotechnol.* **115,** 113–128 (2005).

17. Van Den Biggelaar, M. *et al.* Factor VIII interacts with the endocytic receptor low-density lipoprotein receptor-related protein 1 via an extended surface comprising 'hot-spot' lysine residues. *J. Biol. Chem.* **290,** 16463–16476 (2015).

18. S??nchez, M. C. *et al.* Low-density lipoprotein receptor-related protein-1 (LRP-1) expression in a rat model of oxygen-induced retinal neovascularization. *Exp. Eye Res.* **83,** 1378–1385 (2006).

19. Horn, I. R., Berg, B. M. M. Van Den, Meijden, P. Z. Van Der, Pannekoek, H. & Zonneveld, A. Van. Molecular Analysis of Ligand Binding to the Second Cluster of Complement-type Repeats of the Low Density Lipoprotein Receptor-related Protein. *J. Biol. Chem.* **272,** 13608–13613 (1997).

20. Ranganathan, S. *et al.* Molecular Basis for the Interaction of Low Density Lipoprotein Receptor-related Protein 1 (LRP1) with Integrin {alpha}M{beta}2: IDENTIFICATION OF BINDING SITES WITHIN {alpha}M{beta}2 FOR LRP1. *J. Biol. Chem.* **286,** 30535–30541 (2011).

21. Jensen, J. K., Dolmer, K., Schar, C. & Gettins, P. G. W. Receptor-associated protein (RAP) has two high-affinity binding sites for the low-density lipoprotein receptor-related protein (LRP): consequences for the chaperone functions of RAP. *Biochem. J.* **421,** 273–82 (2009).

22. Andersen, O. M. *et al.* Dominant thermodynamic role of the third independent receptor

binding site in the receptor-associated protein RAP. *Biochemistry* **40,** 15408–15417 (2001).

23. Simonovic, M. *et al.* Calcium coordination and pH dependence of the calcium affinity of ligand-binding repeat CR7 from the LRP. Comparison with related domains from the LRP and the LDL receptor. *Biochemistry* **40,** 15127–15134 (2001).
24. Peyvandi, F., Garagiola, I. & Seregni, S. Future of coagulation factor replacement therapy. *J. Thromb. Haemost.* **11,** 84–98 (2013).
25. Kaufman, R. J., Wasley, L. C. & Dorner, a J. Synthesis, processing, and secretion of recombinant human factor VIII expressed in mammalian cells. *J. Biol. Chem.* **263,** 6352–6362 (1988).
26. Yoo, K. Y. Hemophilia. *Korean J. Pediatr.* **Vol. 49,** 821–829 (2006).
27. Lyu, C. J. Introduction to Coagulation System. *J. Korean Soc. Neonatol.* **18,** 1 (2011).
28. Lacroix-Desmazes, S. *et al.* Dynamics of factor VIII interactions determine its immunologic fate in hemophilia a. *Blood* **112,** 240–249 (2008).
29. Ngo, J. C. K., Huang, M., Roth, D. A., Furie, B. C. & Furie, B. Crystal Structure of Human Factor VIII: Implications for the Formation of the Factor IXa-Factor VIIIa Complex. *Structure* **16,** 597–606 (2008).
30. Lee, D. *et al.* The structure of receptor-associated protein (RAP). *Protein Sci.* **16,** 1628–1640 (2007).
31. Krieger, M. Structures and Functions of Multiligand Lipoprotein Receptors: Macrophage Scavenger Receptors and LDL Receptor-Related Protein (LRP). *Annu. Rev. Biochem.* **63,** 601–637 (1994).
32. Strickland, D. K., Gonias, S. L. & Argraves, W. S. Diverse Roles for the LDL Receptor

Family. *Trends Endocrinol. Metab.* **13,** 66–74 (2002).

33. Bu, G., Geuze, H. J., Strous, G. J. & Schwartz, A. L. 39 kDa receptor-associated protein is an ER resident protein and molecular chaperone for LDL receptor-related protein. *EMBO J.* **14,** 2269–80 (1995).

34. Willnow, T. E., Christ, A. & Hammes, A. Endocytic receptor-mediated control of morphogen signaling. *Development* **139,** 4311–4319 (2012).

35. Willnow, T. E., Armstrong, S. A., Hammer, R. E. & Herz, J. Functional expression of low density lipoprotein receptor-related protein is controlled by receptor-associated protein in vivo. *Proc. Natl. Acad. Sci. U. S. A.* **92,** 4537–41 (1995).

36. Obermoeller, L. M., Warshawsky, I., Wardell, M. R. & Bu, G. Differential functions of triplicated repeats suggest two independent roles for the receptor-associated protein as a molecular chaperone. *J. Biol. Chem.* **272,** 10761–10768 (1997).

37. Fisher, C., Beglova, N. & Blacklow, S. C. Structure of an LDLR-RAP Complex Reveals a General Mode for Ligand Recognition by Lipoprotein Receptors. *Mol. Cell* **22,** 277–283 (2006).

38. Homola, J., Yee, S. S. & Gauglitz, G. Surface plasmon resonance sensors: review. *Sensors Actuators B Chem.* **54,** 3–15 (1999).

39. Wilson, W. D. Ech ight. *Science (80-.).* **295,** 64–65 (2002).

40. Herz, J., Goldstein, J. L., Strickland, D. K., Ho, Y. K. & Brown, M. S. 39-kDa protein modulates binding of ligands to low density lipoprotein receptor-related protein/a2-macroglobulin receptor. *J. Biol. Chem.* **266,** 21232–21238 (1991).

41. Trathnigg, B. Determination of MWD and chemical composition of polymers by

chromatographic techniques. **20,** 615–650 (1995).

42. Hong, P., Koza, S. & Bouvier, E. S. P. A review size-exclusion chromatography for the analysis of protein biotherapeutics and their aggregates. *J. Liq. Chromatogr. Relat. Technol.* **35,** 2923–2950 (2012).

43. Lebowitz, J., Lewis, M. S. & Schuck, P. Modern analytical ultracentrifugation in protein science: A tutorial review. *Protein Sci.* **11,** 2067–2079 (2009).

44. Yamamoto, K. *et al.* Low density lipoprotein receptor-related protein 1 (LRP1)-mediated endocytic clearance of a disintegrin and metalloproteinase with thrombospondin motifs-4 (ADAMTS-4): Functional differences of non-catalytic domains of ADAMTS-4 and ADAMTS-5 in LRP1 binding. *J. Biol. Chem.* **289,** 6462–6474 (2014).

45. Makarova, A. *et al.* The LDL receptor-related protein can form homo-dimers in neuronal cells. *Neurosci. Lett.* **442,** 91–95 (2008).

46. Young, P. A., Migliorini, M. & Strickland, D. K. Evidence that factor VIII forms a bivalent complex with the Low Density Lipoprotein (LDL) Receptor-related Protein 1 (LRP1): Identification of cluster IV on LRP1 as the major binding site. *J. Biol. Chem.* **291,** 26035–26044 (2016).

47. Andersen, C. B. F. & Moestrup, S. K. How calcium makes endocytic receptors attractive. *Trends Biochem. Sci.* **39,** 82–90 (2014).

48. Huang, W., Dolmer, K. & Gettins, P. G. NMR solution structure of complement-like repeat CR8 from the low density lipoprotein receptor-related protein. *J. Biol. Chem.* **274,** 14130–14136 (1999).

49. Dolmer, K., Huang, W. & Gettins, P. G. NMR solution structure of complement-like repeat

CR3 from the low density lipoprotein receptor-related protein. Evidence for specific binding to the receptor binding domain of human alpha(2)-macroglobulin. *J. Biol. Chem.* **275,** 3264–3269 (2000).